ACS SENSORS

Article

Detection and quantification of label-free infectious adenovirus using a switch-on cell-based fluorescent biosensor

Miguel Ricardo Guerreiro, Daniela Filipa Freitas, Paula M. Alves, and Ana Sofia Coroadinha

ACS Sens., **Just Accepted Manuscript** • DOI: 10.1021/acssensors.9b00489 • Publication Date (Web): 22 May 2019

Just Accepted

is published by the American Chemical Society. 1155 Sixteenth Street N.W., Washington, DC 20036

Detection and quantification of label-free infectious adenovirus using a switch-on cell-based fluorescent biosensor

Miguel Ricardo Guerreiro[†,‡], Daniela Filipa Freitas[†,‡], Paula Marques Alves[†,‡] and Ana Sofia Coroadinha[†,‡,§,*]

[†] iBET, Instituto de Biologia Experimental e Tecnológica, Apartado 12, 2781-901 Oeiras, Portugal

[‡] Instituto de Tecnologia Química e Biológica António Xavier, Universidade Nova de Lisboa, Av. da República, 2780-157 Oeiras, Portugal

[§] The Discoveries Centre for Regenerative and Precision Medicine, NOVA University Lisbon, Portugal

KEYWORDS: Cell-based bioassay; Fluorescent biosensor; Label-free; Virus; Quantification; Protease; Intein

ABSTRACT: Reliable and fast viral detection and quantification protocols are a requirement for the advance of basic research and clinical approaches with wild type or recombinant viruses. However, available cell-based assays are either time-consuming or require labeled viral particles, which may alter virus biology or pose safety issues in clinical applications. As Adenoviruses constitute a major healthcare burden but also, when engineered, widely used vectors in vaccination and gene and oncolytic therapies, herein we developed a genetically encoded switch-on fluorescent biosensor consisting on a cyclized Green Fluorescent Protein – cVisensor – with an adenoviral protease cleavable site as a switch. After initial sensor optimization (35% increase in performance), whole-cell biosensors were established – by stably expressing cVisensor in mammalian cells – and used for live-cell monitoring of adenovirus infection as the intracellular biosensor is specifically activated by the viral protease. A rapid flow cytometry-based bioassay using cVisensor cells was established 48 hours post-infection, showing an estimated limit of detection of 10^5 infectious particles per mL, in-line with previously reported flow cytometry assays requiring labeled virus, and significantly faster than standard plaque-forming assays requiring up to 14 days. cVisensor was also successfully applied in the detection of HIV-1 protease activity, validating its wider potential for the detection of other viruses. Overall, this work presents a fast and easy method for detection and quantification of label-free infectious virus, allowing the establishment of new biosensing platforms for basic research in virology and biotechnological applications of recombinant virus biopharmaceuticals.

Clinical applications making use of wild type virus or recombinant virus require reliable and fast detection and quantification assays. This is an important concern in vaccine and antiviral drug development, where infectious virus quantification is needed to evaluate viral replication inhibition, as well as for gene therapy protocols, where different dosages can lead to therapeutic benefits or severe adverse effects.[1]

Adenoviruses are non-enveloped, linear double-stranded DNA viruses with more than 50 distinct serotypes identified (reviewed in San Martín[2]). They have been object of intense study in virology – as a model for eukaryotic cellular processes such as splicing and apoptosis – and in clinical research – since are responsible for a growing number of acute respiratory, gastrointestinal and ocular infections.[3] Adenoviruses have been modified to be used as gene therapy vectors and vaccines due to their attractive features such as the ability to infect non-dividing cells and high packaging capacity and transduction efficiency. As a result, adenoviral-based vectors have become the most widely used vector in gene therapy clinical trials (reviewed in Kotterman et al.[4]) and the first human gene therapy product to enter into the market.[5] Several titration methods for Adenoviruses and adenoviral vectors have been developed, and can be divided in two major categories: physical/non-functional and biological/functional assays. The former quantify total number of physical viral particles by optical absorbance at 260 nm,[6] electron microscopy,[7] nanoparticle tracking analysis[8] or more modern approaches such as electrochemical impedance spectroscopy[9] or surface plasmon resonance imaging.[10]

However, most of the physical assays rely on highly purified viral samples, expensive apparatus, and overestimate functional vector titer. In contrast, functional assays quantify infectious viral particles, being plaque-forming assay[11] and tissue culture infectious dose-50 (TCID50)[12] the "gold standard" methods. However, not all viruses create clear plaques nor induce cytopathic effects.[13] Additionally, these assays are time-consuming (lasting up to 14 days) and operator error-prone. Alternative available methods include fluorescent focus assays,[14] quantitative PCR,[15] immunostaining,[16,17] or rely on labeled virus expressing viral-genome coupled reporter genes such as Green Fluorescent Protein (GFP).[18,19] Although such protocols might be relatively fast and easy to perform, they demand pre-treatment of samples, use of expensive antibodies, or require virus modification. Moreover, vectors containing reporter genes are not allowed in gene therapy protocols due to safety issues and the new generation vaccines tends to be based on genome-free virus-like particles. As so, there is an urgent need of new systems for the detection and quantification of label-free infectious virus. One strategy to achieve this is through the detection of viral enzymatic activity in host cells. As many other viruses (reviewed in Tong[20]), Adenoviruses encode a protease – adenoviral protease (AVP), also known as Adenain[21,22] – essential in viral replication, catalyzing the processing of viral polyproteins and maturation of precapsids. A number of viral protease-dependent sensors have been developed, whether by measurement of luciferase[23,24] or secreted alkaline phosphatase,[25] or by relocalization[26] or switch-on[27,28] of fluorescent proteins. However, they require laborious fluorescence image analysis, lack throughput, and/or are limited to detection but not quantification of virus.

Herein, we report the development of a genetically encoded switch-on fluorescent biosensor – cVisensor, cyclized viral sensor. The proposed biosensor consists on a structurally distorted GFP by means of protein cyclization promoted by the efficient *Nostoc punctiforme* DnaE intein (*Npu* DnaE).[29] Addition of an AVP cleavable sequence into the biosensor allowed relief of the distortion and subsequent fluorescence emission. HEK-293 sensor cells – stably expressing cVisensor – were used for live-cell monitoring of adenovirus infection and for the establishment of a reproducible flow cytometry-based bioassay for quantification of label-free infectious adenovirus 2 days post-infection. This is considerably faster than standard plaque-forming assays requiring up to 14 days. Moreover, as a genetically encoded biosensor, cVisensor can be expressed in other cell types and easily adapted for detection of other viral proteases, as showed herein for detection of HIV-1 proteolytic activity.

EXPERIMENTAL SECTION

Mammalian cell lines. HEK-293 (ATCC® CRL-1573™) and HEK-293T (ATCC® CRL-11268™) were maintained in Dulbecco's Modified Eagle's Medium (DMEM) (Gibco, Paisley, U.K.), supplemented with 10% (v/v) of Fetal Bovine Serum (FBS) (Gibco), at 37 ºC in an incubator with humidified atmosphere of 5% CO_2 in air.

Plasmids. The coding sequence of a cyclized circular permuted superfolder-GFP (cGFP) was designed, using *Npu* DnaE split-intein[30] and to contain the minimal cleavable sequence LRGA*G[21] (asterisk representing scissile bond) for the AVP – backbone cGFP.v1-LRGAG – and synthesized by GenScript (Piscataway, NJ, U.S.A.). Removal of the codon for a methionine amino acid – cGFP.v2-LRGAG; addition of codons for glycine amino acids surrounding the cleavable sequence – cGFP.v3-LRGAG; removal of EcoRI and BamHI restriction sites – cGFP.v4-LRGAG; as well as construction of cGFP.v2 backbone with alternative cleavable sequences for AVP – IVGL*G, MGGR*G, IRGR*G, NTGW*G and EEGE*G (reviewed in Mangel and San Martín[31]) or HIV-1 protease – GIF*LET[32] – were performed by site-directed PCR mutation. The coding sequence of AVP in fusion with the 11-residue peptide from the C-terminus of precursor protein VI (pVIc) with a MVGL*G cleavable sequence[33] was synthesized (GenScript) and used as template for construction of the inactive mutant C104G/C122G[21] – mutAVP – by site-directed PCR mutation. All constructions were inserted into a modified pRRLSIN.cPPT.PGK-GFP.WPRE plasmid (Addgene plasmid #12252, kindly provided by Didier Trono through the Addgene plasmid repository, Watertown, MA, U.S.A.). Briefly, PGK-GFP was substituted by a CMV promoter driving the expression of the developed constructions and an EMCV IRES, amplified from pIRESGALEO,[34] driving the expression of *Sh ble* gene conferring resistance to Zeocin™, amplified from pMONO-zeo-mcs (Invivogen, San Diego, CA, U.S.A.). Details on the construction of Venus- and mCherry-based cyclized biosensors are provided in Supporting Information.

Biosensors initial characterization. For initial evaluation of the different biosensors backbones and/or cleavable sequences, transient transfections with the genetically encoded biosensors were performed. HEK-293T were seeded at 8 x 10^4 cells/cm² in 24-well plates. Cells were co-transfected 24 hours later with 5 µg of total DNA/10^6 cells, using linear 25 kDa polyethylenimine (PEI; Polysciences Inc., Hirschberg, Germany), with each of the biosensor-coding plasmids and either AVP-coding plasmid, mutAVP-coding plasmid, HIV-1 protease-coding plasmid (psPAX2, Addgene plasmid #12260) or a mock plasmid (control). Forty-eight hours later cells were either: a) observed by fluorescence microscopy (DMI6000, Leica, Wetzlar, Germany); b) assessed by flow cytometry (CyFlow Space, Sysmex Partec GmbH, Görlitz, Germany) (gates set using non-transfected HEK-293T as negative control and the geometric mean GFP fluorescence intensity was measured within the positive gate); c) or analyzed by Western blotting.

HEK-293 cell transduction, selection, and cloning. Stable expression of cGFP biosensors in HEK-293 cells was accomplished by lentiviral transduction. For production of lentiviral stocks, HEK-293T cells were seeded at 8 x 10^4 cells/cm² and transiently co-transfected using PEI with the developed pRRLSIN plasmids coding for the respective cGFP biosensors and pMDLg/pRRE (Addgene plasmid #12251), pMD2.G (Addgene plasmid #12259) and pRSV-Rev (Addgene plasmid #12253).[35] For the transduction, HEK-293 cells seeded at a density of 8 x 10^4 cells/cm² in 6-well plates the day before, were transduced with the produced lentivirus stocks in presence of 8 µg/mL of polybrene (Sigma-Aldrich, St. Louis, MO, U.S.A.) for 48 hours, and selected in 200 µg/mL Zeocin™ (Invivogen) containing medium. Selected populations were characterized as such and cloned by limiting dilution assay.

Stocks of adenoviral vectors. Label-free human recombinant E1-deleted adenovirus serotype 5 (AdV; provided by Dr. Geneviève Libeau, CIRAD-EMVT, Montpellier, France) were used. Viral stocks were prepared by infecting HEK-293 cells and 42 hours later cells were harvested. Crude lysate stocks were obtained after three cycles of freeze-thawing of infected cells and clarification by centrifugation for 10 minutes at 3000 x g. Stocks were further purified by banding twice on CsCl gradients, followed by dessalting. Aliquots of both stocks (crude lysates and purified) were stored at -80 ºC in a cryopreservation solution containing 10 mM Tris-HCl buffer (pH 8), 2 mM $MgCl_2$ and 0.5 M Trehalose.[36] AdV titration was performed by TCID50 in HEK-293 cells and titer was calculated according to the method of Spearman and Karber.[37]

Biosensors activation by adenovirus infection. HEK-293 cells stably expressing cGFP biosensors – populations or cell clones – were characterized by seeding cells at 1 x 10^5 cells/cm² in 24-well plates. After 24 hours, cells were infected with the indicated multiplicity of infection (MOI) by removing the culture medium and adding the AdV suspension prepared in 0.2 mL of non-supplemented DMEM (Gibco). After 1 hour with mild agitation, 0.3 mL of supplemented DMEM were added. At each post-infection time point, cells were either: a) observed by fluorescence microscopy; b) assessed by flow cytometry for geometric mean GFP intensity in live cells (excluding membrane-damaged cells by propidium iodide staining); c) assessed for its permissiveness to AdV infection and replication by titration of AdV productivity in crude lysates; d) or analyzed by Western blotting.

Western blotting. Transiently transfected HEK-293T cells or AdV-infected HEK-293 cVisensor cell clone were lysed in M-PER Mammalian Protein Extraction Reagent (Thermo Scientific, Rockford, IL, U.S.A.) supplemented with cOmplete™ EDTA-free Protease Inhibitor Cocktail (Roche Diagnostics GmbH, Mannheim, Germany). Equal amounts of protein (30 µg) were resolved in 12% (w/v) SDS–PAGE gels (Invitrogen, Carlsbad, CA, U.S.A.) and then transferred to polyvinylidene difluoride membranes. Anti GFP (#2955, 1:1000) and anti Myc-tag (#2278, 1:1000) obtained from Cell Signaling Technology (Danvers, MA, U.S.A.), anti α-tubulin (T6199, 1:5000) (Sigma-Aldrich), and anti β-actin (ab8226, 1:2000) (Abcam, Cambridge, U.K.) were used as primary antibodies. Secondary antibody incubation was performed with HRP-conjugated sheep anti-mouse IgG (NA931V, 1:5000) or donkey anti-rabbit (NA934V, 1:5000) from GE Healthcare (Little Chalfont, U.K.).

Data and statistical analysis. Signal to Noise Ratio (SNR) was used to evaluate biosensor performance. Herein, SNR is given by the ratio between the geometric mean fluorescence intensity (measured by flow cytometry) upon biosensor activation in response to proteolysis (Signal), and the geometric mean fluorescence intensity of mock or non-infected controls (Noise). Data are given as mean ± standard deviation (SD). For statistical comparison on the optimization of sensor backbones and cleavable sequences performance, one-way analysis of variance followed by Tukey's post-hoc test was performed. *P* values < 0.05 were considered statistically significant.

RESULTS AND DISCUSSION

Design of switch-on fluorescent biosensors activated by viruses through proteolytic activity. A genetically encoded switch-on fluorescent biosensor with a viral protease cleavable site as a switch was designed and developed for detection of label-free infectious virus, as depicted in Figure 1. The strategy was based on structural distortion of GFP by means of protein cyclization. Truncated N- and C-termini of GFP were linked with a cleavable sequence recognized by a viral protease. Additionally, new N- and C-termini at GFP residues A154 and D155 were generated and joined with DnaEc and DnaEn fragments, respectively, of the *Npu* DnaE split-intein. Intein-mediated splicing at the natural exteins (residues CFN and AEY) led to cyclization of GFP – hereafter referred as cGFP, cyclized Green Fluorescent Protein – and inhibition of fluorescence emission. Fluorescence is reconstituted once proteolytic cleavage takes place at the cleavable sequence and cGFP is converted to a linear form, able to complete its final maturation and emit fluorescence.

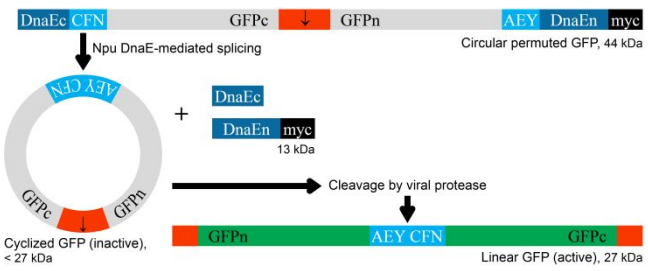

Figure 1. Design of the switch-on fluorescent biosensor. A circular permuted superfolder-GFP (GFP), containing a proteolytic cleavable sequence (red box, arrow representing scissile bond), is cyclized by *Nostoc punctiforme* DnaE split-intein (*Npu* DnaE). Structural distortion inhibits fluorescence emission until viral proteolytic cleavage takes place at the cleavable sequence. Theoretical protein molecular weights (in kDa) are indicated. DnaEc, C-fragment of *Npu* DnaE; CFN, residues of C-extein; GFPc, C-terminal fragment of GFP; GFPn, N-terminal fragment of GFP; AEY, residues of N-extein; DnaEn, N-fragment of *Npu* DnaE; myc, epitope tag derived from c-Myc protein.

Optimization of cyclized biosensors. To assess the feasibility of the proposed strategy, an AVP activation-dependent cGFP biosensor containing LRGA*G residues as cleavable sequence – cGFP.v1-LRGAG – was tested. Co-transfection of HEK-293T cells with plasmids coding cGFP.v1-LRGAG and AVP showed an increase in mean GFP intensity over the negative control (SNR 1.5 ± 0.04, Figure 2A), suggesting sensor activation upon proteolysis.

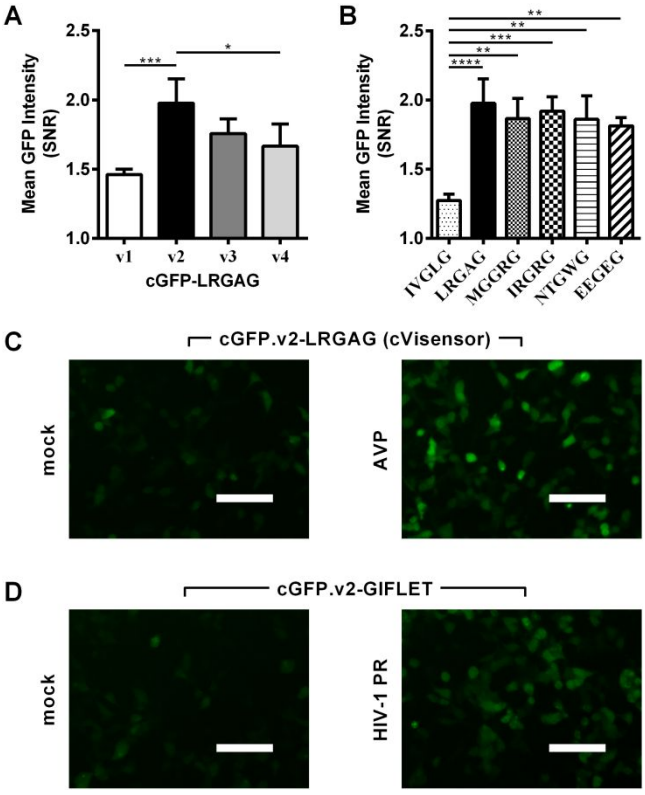

Figure 2. Impact of backbones and cleavable sequences on biosensor performance. GFP signal to noise ratios (SNR) of (A) different cGFP backbones and (B) different cleavable sequences in the optimal cGFP.v2 backbone were assessed by flow cytometry 48 hours after transient co-transfection with a plasmid coding for AVP or a mock plasmid. Data shown as mean ± SD of at least three independent experiments. *P < 0.05, **P < 0.01, ***P < 0.001, ****P < 0.0001. Fluorescence microscopy of (C) cGFP.v2-LRGAG and (D) cGFP.v2-GIFLET 48 hours after co-transfection with plasmids coding the viral proteases (AVP or HIV-1 protease, respectively) or a mock plasmid. Scale bar = 100 μm.

To increase performance of the proposed strategy, the biosensor backbone (amino acid residues supporting the cleavable sequence) was sequentially mutated and evaluated. To avoid a second potential open reading frame leading to expression of non-cyclized GFP, with concomitant increase in background fluorescence, a methionine residue at the beginning of the new N-terminal end of GFP was removed – cGFP.v2-LRGAG. Glycine spacers on each side of LRGA*G were added to evaluate a potential increase in the conformational flexibility and exposure of the cleavable sequence to AVP – cGFP.v3-LRGAG. Additionally, and to evaluate a potential increase in the structural distortion of the biosensor, extra amino acids (resulting from endonuclease restriction sites) (Table S1) were removed. The performed mutations significantly influenced both sensor fluorescence emission (Figure S1) and sensor performance. Indeed, cGFP.v2-LRGAG showed a 35% increase in sensor performance (SNR 2.0 ± 0.2) when compared to the original version (cGFP.v1-LRGAG) (Figure 2A). cGFP.v3-LRGAG (SNR 1.8 ± 0.1) did not significantly differ from other backbones. Finally, cLRGAG.v4-LRGAG led to increased fluorescence emission at the expense of a lower sensor performance (SNR 1.7 ± 0.2). In parallel, a similar sequential optimization approach was followed using Venus fluorescent protein, successfully reported[30] in a strategy for caspase-3 activity detection. However, low sensor performance and fluorescence emission for detection of AVP activity were obtained (Figure S2). Similar results were found when using mCherry as fluorescent protein (SNR 1.2 ± 0.2, n = 3; Figure S3). Taken together, cGFP.v2 was chosen as the best backbone for our fluorescent biosensor.

Different cleavable sequences may lead to different recognition efficiencies by the AVP[21,22,38] as well as induce different structural distortions. Therefore, and alternatively to LRGA*G, the use of cleavable sequences naturally occurring in the adenoviral polyproteins - IVGL*G, MGGR*G, IRGR*G, NTGW*G and EEGE*G – were assessed in the optimal cGFP.v2 backbone. As shown in Figure 2B and Figure S4, different cleavable sequences influenced not only biosensor fluorescence emission but also its performance, with cGFP.v2-IVGLG presenting the lowest fluorescence emission and performance (SNR 1.3 ± 0.05). We hypothesize that prevalence of predominantly hydrophobic amino acids in IVGL*G cleavable sequence had a negative impact in sensor folding and/or cleavable sequence exposure to AVP. On the other hand, EEGE*G has in its composition predominantly hydrophilic amino acids, whereby sensor folding might be less affected by distortion, leading to the observed increase in fluorescence emission. The observed GFP fluorescence emission before sensor's proteolytic activation (Figures S1 and S4) might arise from insufficient structural distortion

of the sensors. As highlighted by the usage of alternative cleavable sequences, a fine balance between structural distortion levels and sensor's fluorescence (before or after activation) may exist, requiring careful optimization and validation. Taken together, these results showed that cGFP.v2-LRGAG – hereafter referred as cVisensor, cyclized viral sensor, for simplicity – was the optimal switch-on fluorescent biosensor for detection of AVP activity (Figure 2C and Table S2).

To assess applicability of the developed strategy in the detection of HIV-1 protease activity, cGFP.v2 backbone with GIF*LET as cleavable sequence showed an increase of almost 2-fold in mean GFP intensity (SNR 1.9 ± 0.2, n = 3; Figure 2D). This result validates the potential to expand the herein developed cVisensor strategy for detection of other protease-containing viruses.

cVisensor validation as an adenoviral protease dependent biosensor. To validate that the increase in GFP intensity results from AVP specific proteolysis, protein extracts from HEK-293T cells transiently co-transfected with cVisensor and either a mock, AVP, or a non-functional AVP (mutAVP) coding-plasmids were analyzed by Western blotting (Figure 3 and Figure S5).

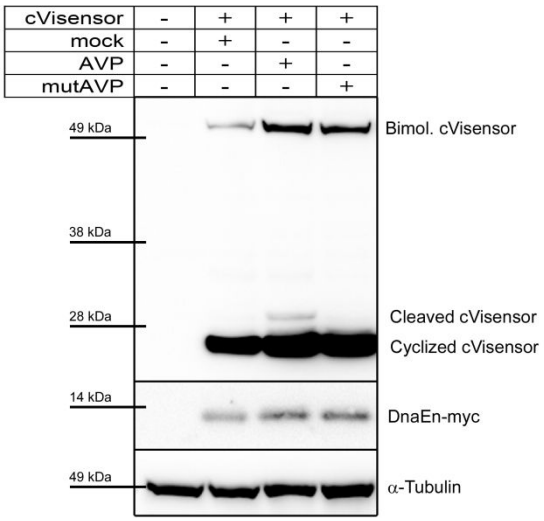

Figure 3. cVisensor validation as an adenoviral protease dependent biosensor. HEK-293T cells were transiently co-transfected with the indicated plasmids. Forty-eight hours later, cell extracts were generated, resolved in 12% (w/v) SDS–PAGE gels, and analyzed by Western blotting. Cleavage of cVisensor was detected (with anti GFP primary antibody) only in the presence of active AVP. Full cyclization was detected (with anti Myc-tag primary antibody) by release of DnaEn-myc (myc-tagged N-fragment of *Nostoc punctiforme* DnaE intein). Molecular weights indicated in the figure correspond to proteins of SeeBlue® Plus2 Pre-Stained Protein Standard (Invitrogen).

Full cyclization by means of *Npu* DnaE was observed by release of the myc-tagged DnaE-fragment (DnaEn-myc, 13 kDa), assembly of the cyclized biosensor (< 27 kDa), and absence of myc-tagged linear biosensor (44 kDa). These results are in accordance with the high rate and efficiency of splicing reaction promoted by *Npu* DnaE.[29] Cleavage of cVisensor was only observed in the presence of active AVP, but not mutAVP, as shown by the appearance of the 27 kDa cleaved cVisensor migrating slower in the gel than its cyclized counterpart. The low ratio of cleaved to cyclized cVisensor may result from partially activated AVP by the presence of pVIc, but not fully activated due to absence of viral DNA. Indeed, AVP is expressed in an almost inactive form, making use of two cofactors for maximal activity: the cleaved 11-residue peptide from the C-terminus of precursor protein VI; and viral DNA.[39] Nevertheless, AVP is also known to be active in the cytoplasm and to cleave both cytokeratin[40] and actin.[41] A protein with < 54 kDa only detected with anti GFP antibody was also observed. This protein may correspond to a cyclized bimolecular biosensor, due to *Npu* DnaE splicing reaction between two cVisensor molecules, which could also work as a biosensor. Taken together, these results show that cVisensor cleavage and activation are specifically dependent on AVP activity.

Biosensor characterization in response to infection by adenoviral vectors. To confirm the results obtained in transient conditions, HEK-293 populations stably expressing the genetically encoded biosensors were established and viral proteolytic cleavage upon AdV infection was evaluated. For the three backbones tested, small differences in terms of biosensor performance in response to AdV infection were observed (Figure 4A). Consistently, cVisensor was the backbone with highest performance. When analyzing the effect of alternative cleavable sequences (Figure 4B), cVisensor showed again to be the best-optimized version of the biosensor for AdV detection, with an SNR of 2.1 ± 0.04 at 48 hours post-infection.

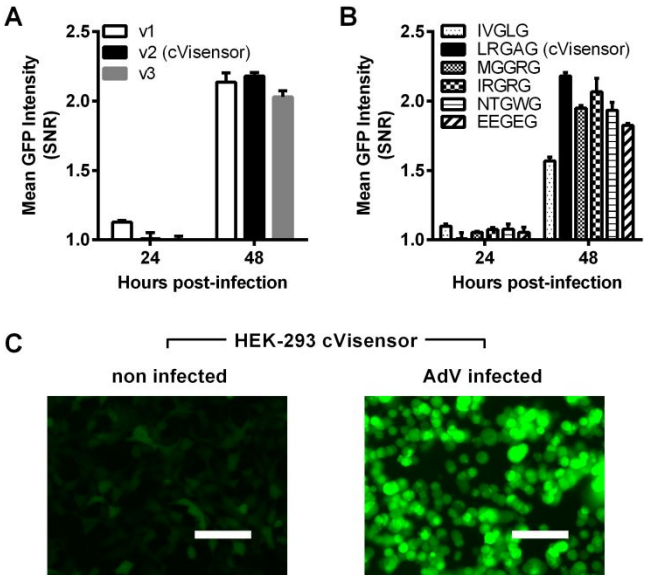

Figure 4. Biosensor characterization in response to adenoviral vector infection. HEK-293 cells stably expressing

biosensors with the (A) indicated cGFP backbones and (B) cGFP.v2 backbone with different cleavable sequences were infected with a stock of crude lysates of adenoviral vectors (AdV) at a multiplicity of infection (MOI) of 5. Biosensor performance, as given by GFP signal to noise ratio (SNR), was measured by flow cytometry. Data shown as mean ± SD of technical triplicates. (C) Fluorescence microscopy of HEK-293 cVisensor cell clone 48 hours post-infection (MOI of 5). Scale bar = 100 µm.

To assess applicability of cVisensor in the establishment of a cellular platform for detection and quantification of AdV, HEK-293 cVisensor cell clones were obtained by limiting dilution. Although different levels of fluorescence emission between cell clones were observed (Figure S6), possibly due to different levels of protein expression, similar SNR performances in response to AdV infection were obtained (data not shown). Therefore, and to achieve higher sensitivity and signal resolution, the cell clone with highest fluorescence intensity was chosen (Figure 4C and Figure S7) to proceed to a detailed characterization.

cVisensor for live-cell monitoring of infection by adenoviral vectors. HEK-293 cVisensor cell clone was further characterized for live-cell monitoring of AdV infection. Permissiveness to AdV infection was evaluated to assess if the presence of additional molecules containing cleavable sequences recognized by AVP had any impact on virus replication. For that, HEK-293 cVisensor cells were infected with AdV. At different time points post-infection, crude lysates were collected to assess infectious AdV production (Figure 5A).

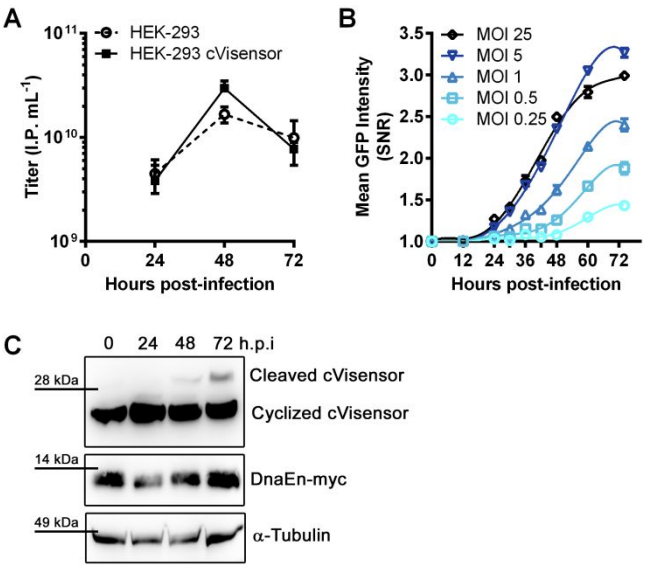

Figure 5. Live-cell monitoring of adenoviral vectors infection. (A) HEK-293 and HEK-293 cVisensor cell clone were infected with a stock of purified adenoviral vectors (AdV) at a multiplicity of infection (MOI) of 5. At the given post-infection time points, permissiveness to viral replication was assessed by quantifying amplified infectious adenovirus particles (I.P.). (B) Kinetic of GFP signal to noise ratio (SNR) increase throughout culture time over increasing MOIs, as assessed by flow cytometry. Data shown as mean ± SD of technical triplicates. (C) Extracts of HEK-293 cVisensor cell clone infected with a stock of purified AdV (MOI of 5) were harvested at 0, 24, 48, and 72 hours post-infection (h.p.i.), resolved in 12% (w/v) SDS–PAGE gels, and analyzed by Western blotting. Cleavage of cVisensor was detected with anti GFP primary antibody. Full cyclization was detected (with anti Myc-tag primary antibody) by release of DnaEn-myc (myc-tagged N-fragment of *Nostoc punctiforme* DnaE intein). Molecular weights indicated in the figure correspond to proteins of SeeBlue® Plus2 Pre-Stained Protein Standard (Invitrogen).

As shown, cVisensor sensor cells supported efficient and similar virus amplification when compared to parental HEK-293 cells. Next, cVisensor cells were infected with increasing MOIs of AdV and subjected to flow cytometry analysis throughout culture time (Figure 5B). At 12 hours post-infection, no SNR increase in infected cells was yet observed. This suggests that the 50-70 molecules of AVP per virus (reviewed in Mangel and San Martín[31]) are not enough to activate the biosensor upon cell entry, thus limiting its applicability to replicative virus. After 12 hours post-infection, an increase in mean GFP intensity of infected cells was seen when compared to non-infected cells. In addition, SNR raised as viral load increased, indicating a good correlation between the two parameters. Western blotting analysis (Figure 5C and Figure S8) confirmed sensor activation as seen by the increase along time of cleaved cVisensor. These results are in agreement with AVP expression and activity kinetics. Indeed, AVP maximal activity in infected cells was reported at 20 hours post-infection[42] with detection by Western blotting in the cytoplasm at 24 hours post-infection.[43] Increase in mean GFP intensity (and SNR) as soon as 24 hours-post infection, despite no cleaved cVisensor being observed by Western blotting, might be explained by the higher sensitivity of our bioassay. The observed low ratio of cleaved to cyclized cVisensor may result from compartmentalization of fully activated AVP (in the nucleus, in presence of pVIc and DNA) and cVisensor (in cytoplasm). As such, we envision that detection of other (cytoplasmatic) viral proteases could lead to higher sensor activation and SNR performance. Collectively, these results validate the applicability of the genetically encoded cVisensor biosensor in the establishment of a live-cell monitoring platform of AdV infection.

cVisensor for quantification of label-free adenoviral vectors. AdV quantification potential was assessed by infecting HEK-293 cVisensor cells with diluted AdV samples and SNR readouts were analyzed by flow cytometry at 48 hours post-infection (Figure 6).

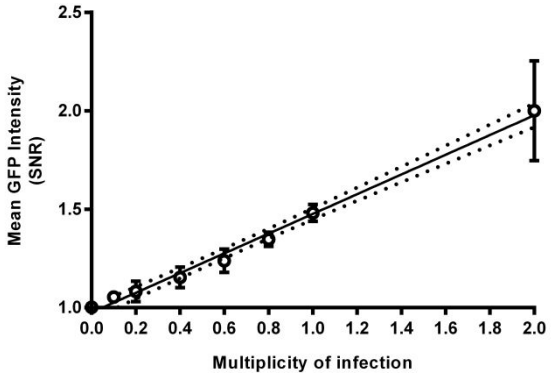

Figure 6. Calibration plot of GFP signal to noise ratio (SNR) as a function of the multiplicity of adenoviral vector infection. HEK-293 cVisensor cell clone was infected with dilutions of a stock of purified adenoviral vectors. Forty-eight hours post-infection, cells were analyzed for SNR by flow cytometry. Linear regression shown by the solid line; 95% confidence intervals shown by the dotted lines. Data shown as mean ± SD of three independent experiments with technical triplicates.

As shown by the calibration plot, for MOIs lower than 2, a linear correlation (r^2 = 0.99) between AdV MOI and SNR readout and a linear regression equation of SNR = 0.50 × MOI + 0.98 were obtained. By measuring SNR, this calibration plot can be used to interpolate unknown MOIs and estimate viral titer using the formula Titer (I.P. mL^{-1}) = (MOI × number of cells at infection × dilution factor)/(volume of infection). Limit of Detection (LOD)[44] was estimated from the linear regression equation to be as low as MOI 0.16, corresponding to 10^5 I.P. mL^{-1} in our experimental conditions. This LOD is in-line with previously developed flow cytometry-based protocols that make use of labeled AdV.[17–19] Since viral titer estimation is influenced by culture working volume, duration of the assay, size of target cells, and diffusion coefficient of AdV,[13] for different experimental conditions it is necessary to perform a calibration curve. LOD might be further reduced by analyzing fluorescence of infected cVisensor sensor cells at later infection time-points. In each case, the large number of cells analyzed by flow cytometry confers robustness to the method, with a maximum intra-assay Coefficient of Variability (CV) of 2% and an inter-assay CV of 9%. As such, cellular platforms providing fast, simple, and reliable live-cell monitoring and quantification of label-free infectious adenovirus can be established with the herein presented cVisensor strategy.

CONCLUSIONS

In summary, we have developed, characterized and validated cVisensor, a switch-on cell-based fluorescent biosensor specifically activated by viral proteolytic activity. Herein, cVisensor enabled the establishment of whole-cell biosensors for live-cell monitoring of AdV infection and reliable quantification of label-free infectious AdV as fast as 2 days post-infection. Although standard plaque-forming assay displays lower LOD, it requires up to 14 days. In contrast, our flow cytometry-based bioassay is significantly faster, which in the context of vector manufacturing enables to reduce timelines and costs for AdV preparation, titration, and characterization. Moreover, cVisensor could be used for antiviral compound screening targeting AVP, tackling the current lack of commercially available specific therapies for adenoviral infections. And as showed for HIV-1 protease, the biosensor here designed can be rapidly modified for detection of other viruses by changing the cleavable sequence specifically recognized by the viral protease. Differences in structure of the active site between proteases and constrains of cleavable sequence length for biosensor performance may nevertheless require optimization and validation for each application. The versatility of the genetically encoded cVisensor can ultimately contribute for the establishment of new biosensing platforms for basic research in virology as well as for manufacturing applications.

ASSOCIATED CONTENT

Supporting Information. Supplementary experimental section; amino acid sequence and fluorescence microscopy images of the biosensors and sensor cells; cVenus sensor performance; full-length Western blots. This material is available free of charge via the Internet at http://pubs.acs.org.

AUTHOR INFORMATION

Corresponding Author

* avalente@ibet.pt

Author Contributions

M.R.G.: conceptualization; experimental design; data collection, and analysis; writing of the manuscript. D.F.F.: data collection. P.M.A.: funding acquisition; review and editing of the manuscript. A.S.C.: conceptualization; funding acquisition; review and editing of the manuscript; supervision; project administration. All authors have given approval to the final version of the manuscript.

Notes

The authors declare no competing financial interest.

ACKNOWLEDGMENT

The authors acknowledge iNOVA4Health Research Unit (LISBOA-01-0145-FEDER-007344), co-funded by Fundação para a Ciência e Tecnologia (FCT) / Ministério da Ciência e do Ensino Superior, through national funds, and by FEDER, under the PT2020 Partnership Agreement; and also FCT for financial support of project LIVES (PTDC/BTM-SAL/30577/2017). M.R.G. acknowledges FCT for the individual grant SFRH/BD/90685/2012.

REFERENCES

(1) Raper, S. E.; Chirmule, N.; Lee, F. S.; Wivel, N. A.; Bagg, A.; Gao, G.; Wilson, J. M.; Batshaw, M. L. Fatal Systemic Inflammatory Response Syndrome in a Ornithine Transcarbamylase Deficient Patient Following Adenoviral Gene

Transfer. *Mol. Genet. Metab.* **2003**, *80* (1–2), 148–158. https://doi.org/10.1016/j.ymgme.2003.08.016.

(2) San Martín, C. Latest Insights on Adenovirus Structure and Assembly. *Viruses* **2012**, *4* (5), 847–877. https://doi.org/10.3390/v4050847.

(3) Lenaerts, L.; De Clercq, E.; Naesens, L. Clinical Features and Treatment of Adenovirus Infections. *Rev. Med. Virol.* **2008**, *18* (6), 357–374. https://doi.org/10.1002/rmv.589.

(4) Kotterman, M. A.; Chalberg, T. W.; Schaffer, D. V. Viral Vectors for Gene Therapy: Translational and Clinical Outlook. *Annu. Rev. Biomed. Eng.* **2015**, *17* (1), 63–89. https://doi.org/10.1146/annurev-bioeng-071813-104938.

(5) Pearson, S.; Jia, H.; Kandachi, K. China Approves First Gene Therapy. *Nat. Biotechnol.* **2004**, *22* (1), 3–4. https://doi.org/10.1038/nbt0104-3.

(6) Maizel, J. V.; White, D. O.; Scharff, M. D. The Polypeptides of Adenovirus. I. Evidence for Multiple Protein Components in the Virion and a Comparison of Types 2, 7A, and 12. *Virology* **1968**, *36* (1), 115–125.

(7) Pinteric, L.; Taylor, J. The Lowered Drop Method for the Preparation of Specimens of Partially Purified Virus Lysates for Quantitative Electron Micrographic Analysis. *Virology* **1962**, *18* (3), 359–371. https://doi.org/10.1016/0042-6822(62)90027-2.

(8) Kramberger, P.; Ciringer, M.; Štrancar, A.; Peterka, M. Evaluation of Nanoparticle Tracking Analysis for Total Virus Particle Determination. *Virol. J.* **2012**, *9* (1), 265. https://doi.org/10.1186/1743-422X-9-265.

(9) Lin, D.; Tang, T.; Jed Harrison, D.; Lee, W. E.; Jemere, A. B. A Regenerating Ultrasensitive Electrochemical Impedance Immunosensor for the Detection of Adenovirus. *Biosens. Bioelectron.* **2015**, *68*, 129–134. https://doi.org/10.1016/j.bios.2014.12.032.

(10) Abadian, P. N.; Yildirim, N.; Gu, A. Z.; Goluch, E. D. SPRi-Based Adenovirus Detection Using a Surrogate Antibody Method. *Biosens. Bioelectron.* **2015**, *74*, 808–814. https://doi.org/10.1016/j.bios.2015.07.047.

(11) Green, M.; Piña, M.; Kimes, R. C. Biochemical Studies on Adenovirus Multiplication. XII. Plaquing Efficiencies of Purified Human Adenoviruses. *Virology* **1967**, *31* (3), 562–565. https://doi.org/10.1016/0042-6822(67)90241-3.

(12) Nielsen, L. K.; Smyth, G. K.; Greenfield, P. F. Accuracy of the Endpoint Assay for Virus Titration. *Cytotechnology* **1992**, *8* (3), 231–236. https://doi.org/10.1007/BF02522040.

(13) Mittereder, N.; March, K. L.; Trapnell, B. C. Evaluation of the Concentration and Bioactivity of Adenovirus Vectors for Gene Therapy. *J. Virol.* **1996**, *70* (11), 7498–7509.

(14) Philipson, L. Adenovirus Assay by the Fluorescent Cell-Counting Procedure. *Virology* **1961**, *15* (3), 263–268. https://doi.org/10.1016/0042-6822(61)90357-9.

(15) Gallaher, S. D.; Berk, A. J. A Rapid Q-PCR Titration Protocol for Adenovirus and Helper-Dependent Adenovirus Vectors That Produces Biologically Relevant Results. *J. Virol. Methods* **2013**, *192* (1–2), 28–38. https://doi.org/10.1016/j.jviromet.2013.04.013.

(16) Bottley, G.; Holt, J. R.; James, N. J.; Blair, G. E. Flow Cytometric Detection of Adenoviruses and Intracellular Adenovirus Proteins. In *Adenovirus Methods and Protocols, Second Edition, Volume 1*; Wold, W. S. M., Tollefson, A. E., Eds.; Humana Press: New Jersey, 2007; Vol. 130, pp 205–214. https://doi.org/10.1385/1-59745-166-5:205.

(17) Weaver, L. S.; Kadan, M. J. Evaluation of Adenoviral Vectors by Flow Cytometry. *Methods* **2000**, *21* (3), 297–312. https://doi.org/10.1006/meth.2000.1010.

(18) Gueret, V.; Negrete-Virgen, J. A.; Lyddiatt, A.; Al-Rubeai, M. Rapid Titration of Adenoviral Infectivity by Flow Cytometry in Batch Culture of Infected HEK293 Cells. *Cytotechnology* **2002**, *38* (1–3), 87–97. https://doi.org/10.1023/A:1021106116887.

(19) Hitt, D. C.; Booth, J. L.; Dandapani, V.; Pennington, L. R.; Gimble, J. M.; Metcalf, J. A Flow Cytometric Protocol for Titering Recombinant Adenoviral Vectors Containing the Green Fluorescent Protein. *Mol. Biotechnol.* **2000**, *14* (3), 197–203. https://doi.org/10.1385/MB:14:3:197.

(20) Tong, L. Viral Proteases. *Chem. Rev.* **2002**, *102* (12), 4609–4626. https://doi.org/10.1021/cr010184f.

(21) Diouri, M.; Keyvani-Amineh, H.; Geoghegan, K. F.; Weber, J. M. Cleavage Efficiency by Adenovirus Protease Is Site-Dependent. *J. Biol. Chem.* **1996**, *271* (51), 32511–32514. https://doi.org/10.1074/jbc.271.51.32511.

(22) Webster, A.; Russell, S.; Talbot, P.; Russell, W. C.; Kemp, G. D. Characterization of the Adenovirus Proteinase: Substrate Specificity. *J. Gen. Virol.* **1989**, *70 (Pt 12* (12), 3225–3234. https://doi.org/10.1099/0022-1317-70-12-3225.

(23) Shekhawat, S. S.; Porter, J. R.; Sriprasad, A.; Ghosh, I. An Autoinhibited Coiled-Coil Design Strategy for Split-Protein Protease Sensors. *J. Am. Chem. Soc.* **2009**, *131* (42), 15284–15290. https://doi.org/10.1021/ja9050857.

(24) Zhou, J.; Wang, D.; Xi, Y.; Zhu, X.; Yang, Y.; Lv, M.; Luo, C.; Chen, J.; Ye, X.; Fang, L.; et al. Assessing Activity of Hepatitis A Virus 3C Protease Using a Cyclized Luciferase-Based Biosensor. *Biochem. Biophys. Res. Commun.* **2017**, *488* (4), 621–627. https://doi.org/10.1016/j.bbrc.2017.05.063.

(25) Iro, M.; Witteveldt, J.; Angus, A. G. N.; Woerz, I.; Kaul, A.; Bartenschlager, R.; Patel, A. H. A Reporter Cell Line for Rapid and Sensitive Evaluation of Hepatitis C Virus Infectivity and Replication. *Antiviral Res.* **2009**, *83* (2), 148–155. https://doi.org/10.1016/j.antiviral.2009.04.007.

(26) Jones, C. T.; Catanese, M. T.; Law, L. M. J.; Khetani, S. R.; Syder, A. J.; Ploss, A.; Oh, T. S.; Schoggins, J. W.; MacDonald, M. R.; Bhatia, S. N.; et al. Real-Time Imaging of Hepatitis C Virus Infection Using a Fluorescent Cell-Based Reporter System. *Nat. Biotechnol.* **2010**, *28* (2), 167–171. https://doi.org/10.1038/nbt.1604.

(27) Garcia-Rivera, J. A.; Lin, K.; Hopkins, S.; Gregory, M. A.; Wilkinson, B.; Gallay, P. A. Development of a Flow Cytometry Live Cell Assay for the Screening of Inhibitors of Hepatitis C Virus (HCV) Replication. *Open Virol. J.* **2012**, *6* (1), 97–102. https://doi.org/10.2174/1874357901206010097.

(28) Zhao, F.; Zhao, T.; Deng, L.; Lv, D.; Zhang, X.; Pan, X.; Xu, J.; Long, G. Visualizing the Essential Role of Complete Virion Assembly Machinery in Efficient Hepatitis C Virus Cell-to-Cell Transmission by a Viral Infection-Activated Split-Intein-Mediated Reporter System. *J. Virol.* **2017**, *91* (2), e01720-16. https://doi.org/10.1128/JVI.01720-16.

(29) Iwai, H.; Züger, S.; Jin, J.; Tam, P.-H. Highly Efficient Protein Trans-Splicing by a Naturally Split DnaE Intein from Nostoc Punctiforme. *FEBS Lett.* **2006**, *580* (7), 1853–1858. https://doi.org/10.1016/j.febslet.2006.02.045.

(30) Zhang, J.; Wang, X.; Cui, W.; Wang, W.; Zhang, H.; Liu, L.; Zhang, Z.; Li, Z.; Ying, G.; Zhang, N.; et al. Visualization of Caspase-3-like Activity in Cells Using a Genetically Encoded Fluorescent Biosensor Activated by Protein Cleavage. *Nat. Commun.* **2013**, *4* (1), 2157. https://doi.org/10.1038/ncomms3157.

(31) Mangel, W. F.; San Martín, C. Structure, Function and Dynamics in Adenovirus Maturation. *Viruses* **2014**, *6* (11), 4536–4570. https://doi.org/10.3390/v6114536.

(32) Beck, Z. Q.; Hervio, L.; Dawson, P. E.; Elder, J. H.; Madison, E. L. Identification of Efficiently Cleaved Substrates for

HIV-1 Protease Using a Phage Display Library and Use in Inhibitor Development. *Virology* **2000**, *274* (2), 391–401. https://doi.org/10.1006/viro.2000.0420.

(33) Balakirev, M. Y.; Jaquinod, M.; Haas, A. L.; Chroboczek, J. Deubiquitinating Function of Adenovirus Proteinase. *J. Virol.* **2002**, *76* (12), 6323–6331. https://doi.org/10.1128/JVI.76.12.6323-6331.2002.

(34) Coroadinha, A. S.; Schucht, R.; Gama-Norton, L.; Wirth, D.; Hauser, H.; Carrondo, M. J. T. The Use of Recombinase Mediated Cassette Exchange in Retroviral Vector Producer Cell Lines: Predictability and Efficiency by Transgene Exchange. *J. Biotechnol.* **2006**, *124* (2), 457–468. https://doi.org/10.1016/j.jbiotec.2006.01.037.

(35) Dull, T.; Zufferey, R.; Kelly, M.; Mandel, R. J.; Nguyen, M.; Trono, D.; Naldini, L. A Third-Generation Lentivirus Vector with a Conditional Packaging System. *J. Virol.* **1998**, *72* (11), 8463–8471.

(36) Cruz, P. E.; Silva, A. C.; Roldão, A.; Carmo, M.; Carrondo, M. J. T.; Alves, P. M. Screening of Novel Excipients for Improving the Stability of Retroviral and Adenoviral Vectors. *Biotechnol. Prog.* **2006**, *22* (2), 568–576. https://doi.org/10.1021/bp050294y.

(37) Darling, A. J.; Boose, J. A.; Spaltro, J. Virus Assay Methods: Accuracy and Validation. *Biologicals* **1998**, *26* (2), 105–110. https://doi.org/10.1006/biol.1998.0134.

(38) Ruzindana-Umunyana, A.; Imbeault, L.; Weber, J. M. Substrate Specificity of Adenovirus Protease. *Virus Res.* **2002**, *89* (1), 41–52. https://doi.org/10.1016/S0168-1702(02)00111-9.

(39) Mangel, W. F.; McGrath, W. J.; Toledo, D. L.; Anderson, C. W. Viral DNA and a Viral Peptide Can Act as Cofactors of Adenovirus Virion Proteinase Activity. *Nature* **1993**, *361* (6409), 274–275. https://doi.org/10.1038/361274a0.

(40) Chen, P. H.; Ornelles, D. A.; Shenk, T. The Adenovirus L3 23-Kilodalton Proteinase Cleaves the Amino-Terminal Head Domain from Cytokeratin 18 and Disrupts the Cytokeratin Network of HeLa Cells. *J. Virol.* **1993**, *67* (6), 3507–3514.

(41) Brown, M. T.; Mangel, W. F. Interaction of Actin and Its 11-Amino Acid C-Terminal Peptide as Cofactors with the Adenovirus Proteinase. *FEBS Lett.* **2004**, *563* (1–3), 213–218. https://doi.org/10.1016/S0014-5793(04)00285-6.

(42) Rashid Bhatti, A.; Weber, J. Protease of Adenovirus Type 2: Partial Characterization. *Virology* **1979**, *96* (2), 478–485. https://doi.org/10.1016/0042-6822(79)90105-3.

(43) Webster, A.; Leith, I. R.; Hay, R. T. Activation of Adenovirus-Coded Protease and Processing of Preterminal Protein. *J. Virol.* **1994**, *68* (11), 7292–7300.

(44) Armbruster, D. A.; Pry, T. Limit of Blank, Limit of Detection and Limit of Quantitation. *Clin. Biochem. Rev.* **2008**, *29 Suppl 1* (August), S49-52.

For Table of Contents Only

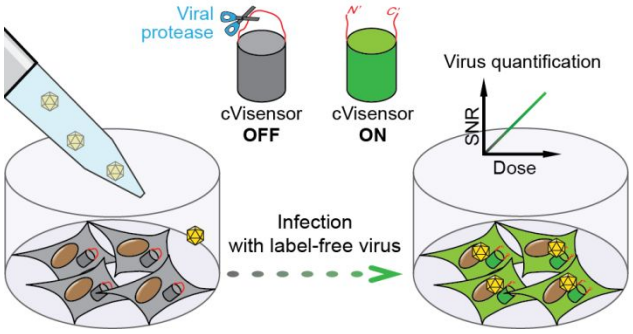
Viral protease
cVisensor OFF
cVisensor ON
N
C
Virus quantification
SNR
Dose
Infection with label-free virus